STM JOURNALS

Trends in
Electrical Engineering

https://journals.stmjournals.com/tee

ISSN: 2249-4774 (Online)
ISSN: 2321-4260 (Print)
Volume 14, Issue 3, 2024
September—December
DOI (Journal): 10.37591/TEE

Research TEE

# Prediction and Evaluation of Photovoltaic Panel Performance for Low Solar Radiation Concentration and Variable Topology

Carlos Armenta-Déu[1,]*, Juan Aguirre[2]

***Abstract***

*This paper studies and analyzes the performance of photovoltaic (PV) panels for a flat-side mirror solar radiation low-concentration design. The system consists of two side mirrors concentrating surface that reflects solar radiation onto the PV panel area, increasing the solar radiation flux up to 177% regarding solar radiation peak at the Earth's surface. Three PV panel configurations are analyzed: conventional, a PV panel with attached phase change material (PV-PCM), and a PV with PCM and heat sink (PV-PCM-HS). For a classical configuration operating under concentrated solar radiation, the power increases by 79.4%. If we remove generated heat using a PCM or PCM and heat sink, the power rises to 115.7% and 152.2%, respectively. The paper develops a new method to predict PV panel output power for variable solar concentration and configurations within 95% minimum agreement. The evaluation of PV panel output power using the developed theoretical algorithm is within 98.6% accuracy, on average.*

**Keywords:** Concentrated solar radiation, photovoltaic panel performance, power increase, efficiency improvement, electric and heat generation

## INTRODUCTION

Photovoltaic (PV) energy represents a reliable solution to replace fossil fuels with renewable energies. The high costs, low energy density of solar radiation and PV panel efficiency are the main barriers to the global implementation of this technology [1–6]. Many studies focus on developing new ways to increase the PV panel output power, increase efficiency, or improve global performance by reducing temperature effects [6–9]. Some efforts aim to raise output power by increasing solar radiation density in the PV panel area through concentration devices [10, 11]. This configuration, however, suffers from solar tracking dependence and temperature raising, which reduces the panel efficiency [12]. Alternative solutions arise from the low-concentrating devices application, which moderately raises the solar radiation flux and increases the PV panel output power [13–15]. The concentration device also enlarges the PV array size and increases the cost. Besides, in large PV installations, concentration devices may shade adjacent panels if not properly arranged, thus reducing the global efficiency and limiting the output power [16–21]. Therefore, the solar radiation concentration systems implementation for PV applications has never represented a reliable solution for PV generation increase.

In past decades, researchers have published new designs for concentrated solar radiation PV systems aiming to solve the traditional problems affecting this technology; among them, static structures with no solar tracking are shown as a solution to avoid dependence on mechanical devices [22–25]. This

***Author for Correspondence**
Carlos Armenta-Déu
E-mail: Cardeu@fis.ucm.es

[1,2]Faculty of Physical Sciences, Complutense University of Madrid, 28040 Madrid, Spain

Received Date: August 20, 2024
Accepted Date: August 27, 2024
Published Date: September 05, 2024

**Citation:** Carlos Armenta-Déu, Juan Aguirre. Prediction and Evaluation of Photovoltaic Panel Performance for Low Solar Radiation Concentration and Variable Topology. Trends in Electrical Engineering. 2024; 14(3): 14–25p.

configuration allows collecting solar radiation in a relatively wide solar angle range, increasing solar flux onto the PV panel area and generating higher output power. Although the solar radiation concentration structure continuously suffers from larger size, which reduces available space for PV panels, it reduces the initial investment supplying extra energy at a relatively low cost. The new configuration is practical for places where PV panel density is not relevant, but the maximum power at minimum cost is critical.

This work is oriented towards this line of development, introducing a system with a low solar concentration index at a minimum cost, which allows reaching a power level double that of a conventional panel with a simple and easy-to-acquire structure.

## THEORETICAL BASIS

Power generation in PV panels depends on solar radiation flux and cell efficiency; mathematically:

$$P_{FV} = \eta G S \tag{1}$$

where $G$ is the solar radiation flux, $S$ is the PV array surface, and $\eta$ the cell efficiency.

If solar radiation concentrates, photovoltaic output power becomes:

$$P_{FV} = C_x \eta G S \tag{2}$$

where $C_x$ is the concentration ratio, defined as:

$$C_x = A_{ap} / A_{rec} \tag{3}$$

$A_{ap}$ and $A_{rec}$ account for the concentrator aperture and receiver area.

Because the panel heats with increasing solar radiation [26, 27], the efficiency reduces according to the expression:

$$\eta(T) = \eta(T_o)\left[1 + \left(\frac{1}{\eta}\frac{d\eta}{dT}\right)\left(T_o - T\right)\right] \tag{4}$$

Sub-index $o$ accounts for reference temperature, currently 25ºC.

Expressing efficiency dependence in terms of PV panel parameters:

$$\frac{1}{\eta}\frac{d\eta}{dT} = \frac{1}{V_{OC}}\frac{dV_{OC}}{dT} + \frac{1}{I_{SC}}\frac{dI_{SC}}{dT} + \frac{1}{FF}\frac{dFF}{dT} \tag{5}$$

$V_{OC}$ is the open circuit voltage, $I_{SC}$ is the short circuit current, and $FF$ is the fill factor defined as:

$$FF = \frac{P_M}{V_{OC} I_{SC}} = \frac{V_M I_M}{V_{OC} I_{SC}} \tag{6}$$

Replacing Equation 6 in Equation 5:

$$\frac{1}{\eta}\frac{d\eta}{dT} = \frac{V_{OC} I_{SC}}{V_M I_M}\left(\frac{I_M}{V_{OC} I_{SC}}\frac{dV_M}{dT} + \frac{V_M}{V_{OC} I_{SC}}\frac{dI_M}{dT}\right) \tag{7}$$

Combining Equations 4 and 7:

ISSN: 2249-4774 (Online), ISSN: 2321-4260 (Print)

$$\eta(T)=\eta(T_o)\left[1+\left(\frac{V_{OC}I_{SC}}{V_M I_M}\left(\frac{I_M}{V_{OC}I_{SC}}\frac{dV_M}{dT}+\frac{V_M}{V_{OC}I_{SC}}\frac{dI_M}{dT}\right)\right)(T_o-T)\right] \tag{8}$$

PV panel temperature evolves until reaching the steady state, which depends on the solar radiation and thermal losses coefficient according to [28]:

$$T_{PV}=T_{amb}+\frac{(1-\eta_{PV})G}{U_L} \tag{9}$$

where $\eta_{PV}=\eta(T_o)$.

Replacing in Equation 8:

$$\eta(T)=\eta(T_o)\left[1+\left(\frac{V_{OC}I_{SC}}{V_M I_M}\left(\frac{I_M}{V_{OC}I_{SC}}\frac{dV_M}{dT}+\frac{V_M}{V_{OC}I_{SC}}\frac{dI_M}{dT}\right)\right)\left(\frac{(\eta(T_o)-1)G}{U_L}\right)\right] \tag{10}$$

We consider that the initial PV panel temperature, $T_o$, matches the ambient temperature.

On the other hand, open circuit voltage and short circuit current depend on temperature as:

$$\begin{aligned}I_{SC}(T)&=I_{SC}(T_o)+\alpha_{SC}(T-T_o)\\ V_{OC}(T)&=V_{OC}(T_o)+\beta_{OC}(T-T_o)\end{aligned} \tag{11}$$

Considering the maximum voltage and current show the same temperature dependence as open circuit voltage and short circuit current, which is an accurate approach, we have:

$$\frac{dV_M}{dT}=\beta_{OC}\ ;\quad \frac{dI_M}{dT}=\alpha_{SC} \tag{12}$$

Therefore, Equation 10 converts into:

$$\eta(T)=\eta(T_o)\left[1+\left(\frac{\beta_{OC}}{V_M}+\frac{\alpha_{SC}}{I_M}\right)\frac{G}{U_L}(\eta(T_o)-1)\right] \tag{13}$$

Combining Equations 2 and 13:

$$P_{FV}=C_x GS\eta(T_o)\left[1+\left(\frac{\beta_{OC}}{V_M}+\frac{\alpha_{SC}}{I_M}\right)\frac{G}{U_L}(\eta(T_o)-1)\right] \tag{14}$$

Because the concentration ratio influences the PV panel performance, the term in brackets modifies with the concentration ratio; therefore:

$$P_{FV}=C_x GS\eta(T_o)\frac{\left[1+\left(\frac{\beta_{OC}}{V_M}+\frac{\alpha_{SC}}{I_M}\right)\frac{G}{U_L}(\eta(T_o)-1)\right]_{C_o}}{\left[1+\left(\frac{\beta_{OC}}{V_M}+\frac{\alpha_{SC}}{I_M}\right)\frac{G}{U_L}(\eta(T_o)-1)\right]_{C_x}} \tag{15}$$

Sub-indexes $C_o$ and $C_x$ account for the reference and current case.

Equation 15 does not consider the heat transfer from the PV panel to the PCM, which modifies the PV panel's thermal performance and temperature operation; therefore, we should apply a heat transfer factor to Equation 15, which considers the thermal flow from the panel to PCM. Equation 15 adopts the form:

$$P_{FV} = F_o C_x G S \eta(T_o) \frac{\left[1+\left(\frac{\beta_{OC}}{V_M}+\frac{\alpha_{SC}}{I_M}\right)\frac{G}{U_L}\left(\eta(T_o)-1\right)\right]_{C_o}}{\left[1+\left(\frac{\beta_{OC}}{V_M}+\frac{\alpha_{SC}}{I_M}\right)\frac{G}{U_L}\left(\eta(T_o)-1\right)\right]_{C_x}} \tag{16}$$

where $F_o$ represents the correction factor for the PV panel output power due to the heat transfer.

Equation 15 provides the PV output power as a function of the panel characteristics and solar radiation flux onto the panel surface.

On the other hand, the correction factor depends on the heat transfer, which, on its way, depends on panel temperature and heat transfer mode. Since the panel temperature depends on the solar radiation flux, which depends on the concentration ratio, we may establish a relation between the correction factor and the concentration ratio.

Considering that radiation is the most relevant heat transfer mode for conventional PV panel configuration and that conduction is the principal heat transfer mode when PCM is attached to the PV panel [29], we have:

$$\begin{aligned} \dot{Q}_{cd} &= \frac{\kappa}{e} S\left(T-T_o\right) \\ \dot{Q}_{rad} &= \sigma\varepsilon S\left(T^4-T_o^4\right) \end{aligned} \tag{17}$$

The upper and lower sections of Equation 16 correspond to conduction and radiation heat transfer. Operating in the radiation term:

$$\dot{Q}_{rad} = \sigma\varepsilon S\left(T^4-T_o^4\right) = \sigma\varepsilon S\left(T^2+T_o^2\right)\left(T+T_o\right)\left(T-T_o\right) \tag{18}$$

The conduction to radiation heat transfer ratio is therefore:

$$\frac{\dot{Q}_{cd}}{\dot{Q}_{rad}} = \frac{\kappa}{e\sigma\varepsilon}\frac{1}{\left(T^2+T_o^2\right)\left(T+T_o\right)} = \frac{\kappa}{e\sigma\varepsilon}\frac{1}{aT^3+bT^2+cT+d} \quad \left| \begin{aligned} a &= 1 \\ b &= T_o \\ c &= T_o^2 \\ d &= T_o^3 \end{aligned} \right. \tag{19}$$

Now, expressing the correction factor as a function of the heat transfer ratio:

$$F_o = \left(\frac{k_o}{C_x}\right)^{1/3} \rightarrow k_o = \frac{\dot{Q}_{cd}}{\dot{Q}_{rad}} = \frac{\kappa}{e\sigma\varepsilon}\frac{1}{f(T^3)} \tag{20}$$

**CONCENTRATION RATIO**

The concentration ratio, mathematically defined in Equation 3, varies depending on the size and configuration of the concentrating device. In our case, we designed a new type of concentrator

 

ISSN: 2249-4774 (Online), ISSN: 2321-4260 (Print)

consisting of a U-shape articulated structure with a mirror surface on both sides and the PV panel at the central section (Figure 1a).

Considering a PV panel of length $L$ and width $W$ and side mirrors of identical dimensions, the receiving area is: $A_{rec} = LW$, and the aperture area depends on the mirror side tilt. Since the mirror system is articulated, left- and right-side tilt can be different; this configuration is shown in Figure 1b with left tilt angle as $\gamma$ and right tilt angle as $\alpha$.

The concentrating device collects sun rays from the left to right mirror edge. Because the system operates under linear symmetry, the length is equal for PV panels and side mirrors; therefore, we express the concentration ratio as:

$$C_x = W_{ap} / W_{rec} \tag{21}$$

PV panel width, $W$, defines the receiving width, $W_{rec}$; therefore, $W = W_{rec}$. For the aperture width, we develop the following geometrical analysis:

$$W_{ap} = W + w_r + w_l = W + W\cos\alpha + W\cos\gamma \tag{22}$$

The side tilt angles must fulfill the following conditions:

$$\alpha = \frac{\pi}{2} - \theta_r \; ; \gamma = \frac{\pi}{2} - \theta_l \tag{23}$$

Replacing in Equation 21:

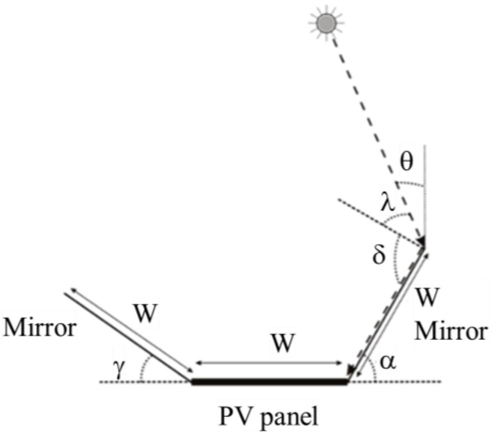


**Figure 1.** (a) Schematic representation of the concentrating device.

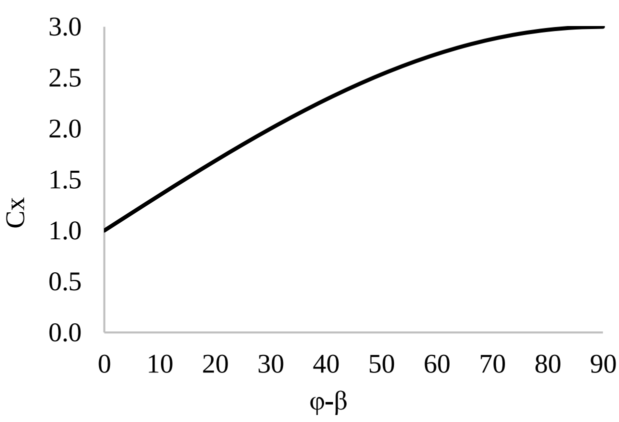


**Figure 1.** (b) Evolution of the concentration ratio versus the apparent tilt angle.

$$C_x = 1 + \cos\alpha + \cos\gamma = 1 + \cos\left(\frac{\pi}{2} - \theta_r\right) + \cos\left(\frac{\pi}{2} - \theta_l\right) = 1 + \sin\theta_r + \sin\theta_l \tag{24}$$

Considering the solar radiation incidence angle is identical for both sides of the concentrating device:

$$C_x = 1 + 2\sin\theta \tag{25}$$

Retrieving the expression for the solar incidence angle [30]:

$$\cos\theta = \sin\delta\sin\phi\sin\beta - \sin\delta\cos\phi\sin\beta\cos\gamma + \cos\delta\cos\phi\cos\beta\cos\omega + \\ + \cos\delta\sin\phi\sin\beta\cos\gamma\cos\omega + \cos\delta\sin\beta\sin\gamma\sin\omega \tag{26}$$

where $\delta$ is the declination, $\Phi$ is the latitude, $\beta$ is the tilt, $\gamma$ is the azimuth, and $\omega$ is the hourly angle.

If we operate for a concentrating device pointing to the Equator, aligned with the local meridian:

$$\cos\theta = \sin\delta\sin\beta\left(\sin\phi - \cos\phi\right) + \cos\delta\left(\cos\phi\cos\beta + \sin\phi\sin\beta\right) \tag{27}$$

Therefore:

$$C_x = 1 + 2\sin\left(\arccos\left[\sin\delta\sin\beta\left(\sin\phi - \cos\phi\right) + \cos\delta\left(\cos\phi\cos\beta + \sin\phi\sin\beta\right)\right]\right) \tag{28}$$

Operating for the whole year and considering average values:

$$C_x = 1 + 2\sin\left(\phi - \beta\right) \tag{29}$$

Representing the concentration ratio as a function of the $\Phi$-$\beta$ angle:

The analysis of Figure 1 shows that the concentration ratio evolves within the 1 to 3 range.

## EXPERIMENTAL DEVICE AND TESTS

The experimental device consists of a 5-W PV panel located in a U-shape structure with mirror sides as shown in Figure 2. As shown in Figure 2, the structure allows varying the sides tilt angle independently; therefore, we can adjust every side tilt to the solar radiation incidence angle. Values shown in Figure 2 are indicative since we can change them according to operating conditions. In our case, we operate for the Madrid location (Φ = 40.68) with a tilt angle of 18º. Applying Equation 23, we obtain a concentration ratio of 1.771, equivalent to a solar radiation of 1771 W/m$^2$.

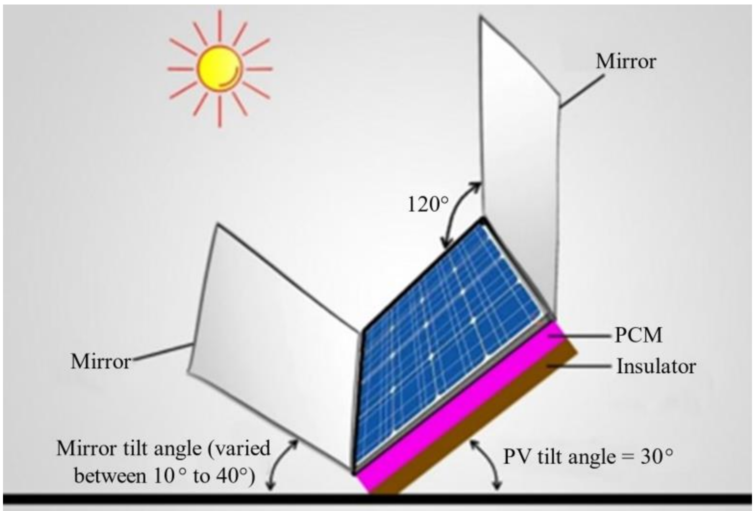


**Figure 2.** Schematic view of the experimental device.

Tests run for tilt angles between 18º and 0º. Table 1 shows the corresponding concentration ratio and solar radiation flux for the running tests. We observe that the experimental solar radiation deviates from the theoretical value of less than 1%. We tested three types of PV panels with the following structures: conventional (type A), PV-PCM (type B), and PV-PCM-HS (type C). The PV-PCM includes a phase change material (PCM) to evacuate generated heat due to concentrated solar radiation, and the PV-PCM-HS adds to the PCM a heat sink (HS) to optimize heat removal.

## EXPERIMENTAL RESULTS

The first group of tests characterizes the PV panel performance through the classic I-V curve. Figures 3–5 show the characterization process for the three panel types, respectively.

**Table 1.** Concentration ratio and solar radiation flux.

| Tilt angle (º) | 18 | 22 | 29 | 38 | 40 |
|---|---|---|---|---|---|
| $C_x$ | 1.771 | 1.641 | 1.405 | 1.094 | 1.024 |
| $G_{th}$ ($W/m^2$) | 1771 | 1641 | 1405 | 1094 | 1024 |
| $G_{exp}$ ($W/m^2$) | 1776 | 1639 | 1411 | 1084 | 1020 |
| Deviation (%) | 0.2 | 0.1 | 0.4 | 0.9 | 0.4 |

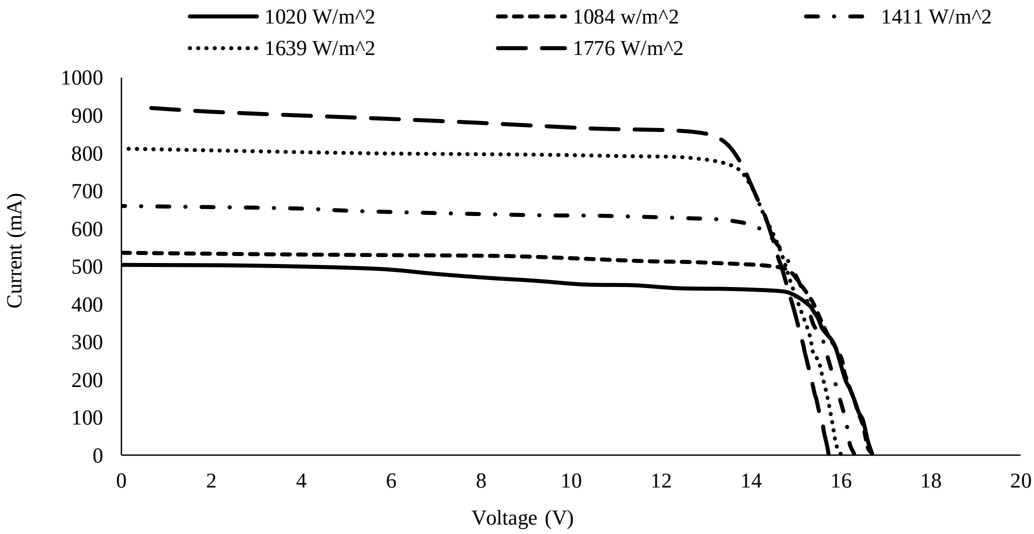


**Figure 3.** I-V curve for photovoltaic (PV) panel type A.

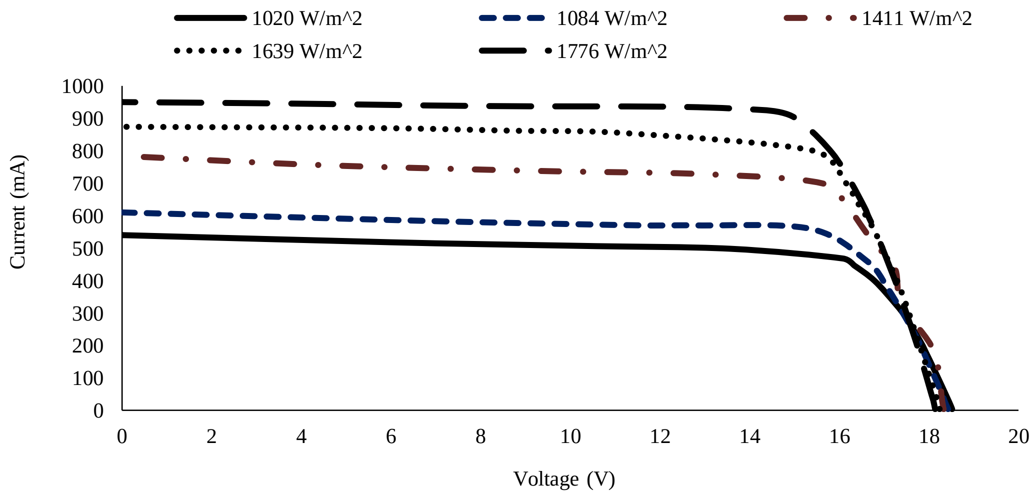


**Figure 4.** I-V curve for photovoltaic (PV) panel type B.

It looks like the maximum current for the various concentration ratio follows a linear pattern; therefore, we correlate the $I_M$ values to a right line for the three PV panel type, according to the expression:

$$I_M = aC_x + b \tag{30}$$

Table 2 shows the correlation coefficients for different PV panel types.

Applying the correlation coefficient from Table 2 to Equation 24, we obtain the maximum current for the corresponding panel type as a function of the concentration ratio.

Following the tests run under specified operating conditions, we obtain the output power for every panel type. Figures 6–8 show the experimental test results. Black dots represent the maximum power point (MPP).

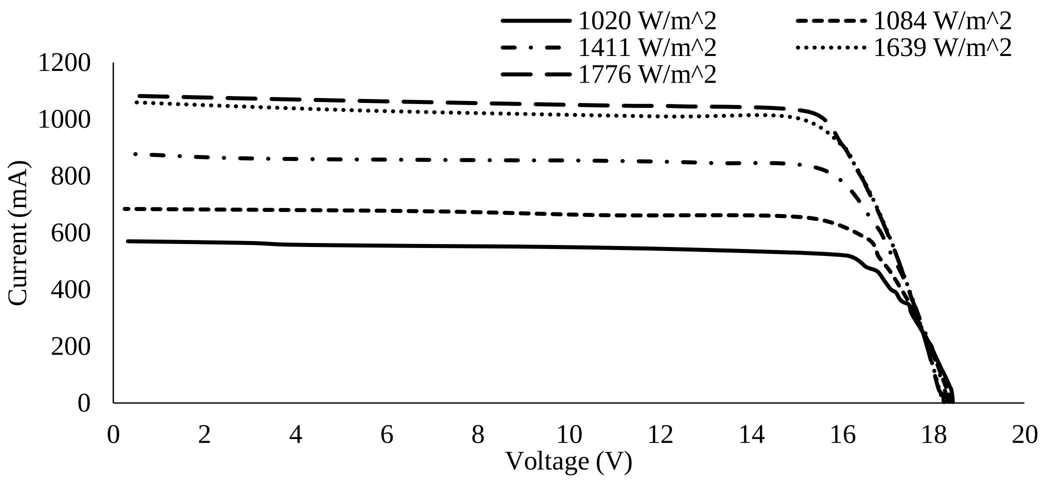


**Figure 5.** I-V curve for photovoltaic (PV) panel type C.

**Table 2.** Correlation of the photovoltaic (PV) panel maximum current for different PV panel types.

| Panel Type | A | B | C |
|---|---|---|---|
| A | 0.5384 | 0.5552 | 0.6652 |
| B | -0.1114 | -0.0809 | -0.1144 |
| $R^2$ | 0.989 | 0.980 | 0.973 |

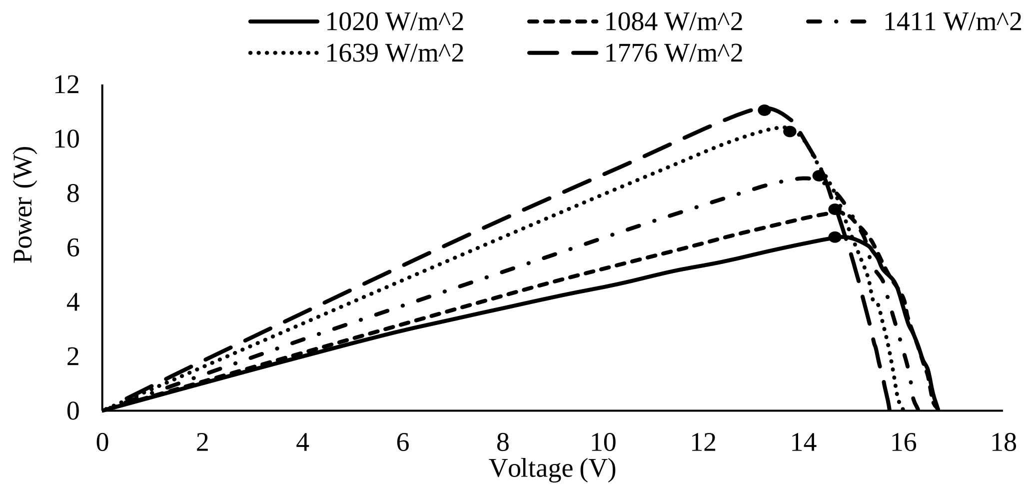


**Figure 6.** Output power for photovoltaic (PV) panel type A for variable solar radiation flux.

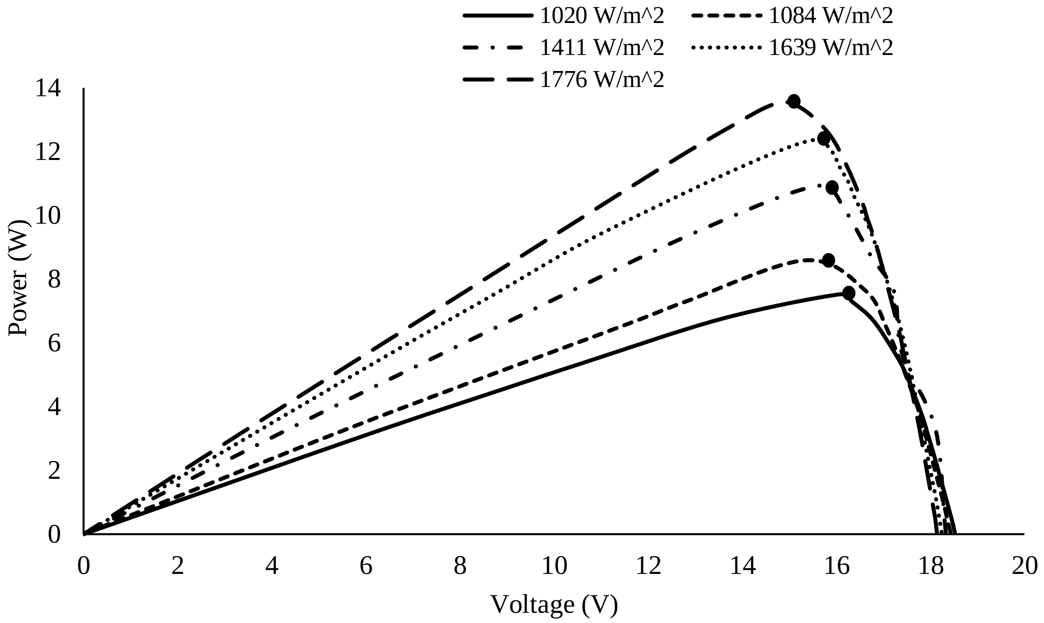


**Figure 7.** Output power for photovoltaic (PV) panel type B for variable solar radiation flux.

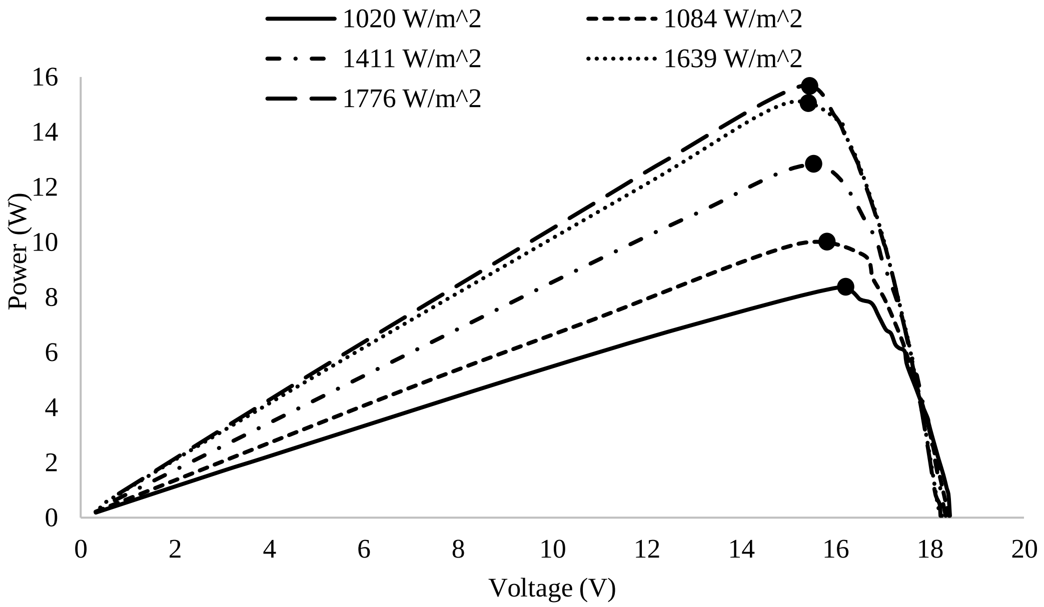


**Figure 8.** Output power for photovoltaic (PV) panel type C for variable solar radiation flux.

**Table 3.** Values of coefficient $k_o$ for the photovoltaic (PV) panel tested configuration.

| Configuration | $k_o$ |
|---|---|
| PV-PCM | 4.657 |
| PV-PCM-HS | 8.103 |

Since coefficient $k_o$ depends on PV panel configuration, we determine the value for the PV-PCM and PV-PCM-HS configurations, resulting in (Table 3).

We compare experimental data with theoretical values to evaluate the prediction accuracy. Table 4 shows the comparison results. We observe the good agreement between theoretical prediction and experimental results, proving the validity of the developed algorithm in Equation 16.

**Table 4.** Photovoltaic (PV) panel output power for variable concentration ratio and configuration.

| | Configuration | | | | | | | | |
|---|---|---|---|---|---|---|---|---|---|
| | *PV* | | | *PV-PCM* | | | *PV-PCM-HS* | | |
| $C_x$ | *Th.* | *Exp.* | *Dev.* | *Th.* | *Exp.* | *Dev.* | *Th.* | *Exp.* | *Dev.* |
| 1.024 | 6.34 | 6.36 | 0.3 | 7.82 | 7.51 | 3.9 | 8.05 | 8.34 | 3.6 |
| 1.094 | 6.93 | 7.24 | 4.4 | 8.26 | 8.57 | 3.7 | 9.24 | 9.68 | 4.8 |
| 1.405 | 8.20 | 8.54 | 4.2 | 10.40 | 10.85 | 4.3 | 12.29 | 12.79 | 4.0 |
| 1.641 | 10.44 | 10.36 | 0.8 | 12.35 | 12.39 | 0.3 | 15.27 | 15.02 | 1.6 |
| 1.771 | 11.07 | 11.10 | 0.3 | 13.47 | 13.53 | 0.4 | 16.26 | 15.65 | 3.8 |

Data for theoretical (Th.) and experimental (Exp.) output power are in watts (W); deviation (Dev.) is represented as percentage (%).

We observe the good agreement between theoretical values and experimental data within a minimum 95% accuracy, proving the validity of the proposed method to evaluate the effects of concentration ratio and PV panel configuration on the output power.

## CONCLUSIONS

New theoretical approach for determining the output power for photovoltaic panels operating under low concentrated solar radiation is proposed. The theoretical development results in an algorithm that predicts the PV panel output power within 98.6% accuracy, on average, for concentration ratios up to 1.771. For a classical configuration operating under concentrated solar radiation, the power increases by 79.4%. If we remove generated heat using a PCM or PCM and heat sink, the power rises to 115.7% and 152.2%, respectively.

The theoretical study applies to different panel configurations, classical, panel with attached PCM (PV-PCM), and panel with PCM and heat sink (PV-PCM-HS). The analysis shows a good agreement between theoretical results and experimental data, higher than 95% in all cases.

The good agreement between theoretical approach and experimental values proves the validity of the proposed method for evaluating the PV panel output power under variable concentrated solar radiation and panel configuration.

The developed methodology considers the temperature effects and the heat transfer from the PV panel to the environment or PCM, allowing to apply this methodology to any PV configuration under variable operating conditions.

## REFERENCES

1. Karakaya E, Sriwannawit P. Barriers to the adoption of photovoltaic systems: the state of the art. Renew Sustain Energy Rev. 2015; 49: 60–66.
2. Agathokleous RA, Kalogirou SA. Status, barriers and perspectives of building integrated photovoltaic systems. Energy. 2020; 191: 116471.
3. Nurwidiana N. Barriers to adoption of photovoltaic system: a case study from Indonesia. J Indus Eng Educ. 2023; 1 (1): 80–89.
4. Lo K, Mah DNY, Wang G, Leung MK, Lo AY, Hills P. Barriers to adopting solar photovoltaic systems in Hong Kong. Energy Environ. 2018; 29 (5): 649–663.
5. Manju S, Sagar N. Progressing towards the development of sustainable energy: a critical review on the current status, applications, developmental barriers and prospects of solar photovoltaic systems in India. Renew Sustain Energy Rev. 2017; 70: 298–313.
6. Singh GK. Solar power generation by PV (photovoltaic) technology: a review. Energy. 2013; 53: 1–13.

 

7. Tyagi VV, Rahim NA, Rahim NA, Jeyraj A, Selvaraj L. Progress in solar PV technology: research and achievement. Renew Sustain Energy Rev. 2013; 20: 443–461.
8. Parida B, Iniyan S, Goic R. A review of solar photovoltaic technologies. Renew Sustain Energy Rev. 2011; 15 (3): 1625–1636.
9. Razykov TM, Ferekides CS, Morel D, Stefanakos E, Ullal HS, Upadhyaya HM. Solar photovoltaic electricity: current status and future prospects. Solar Energy. 2011; 85 (8): 1580–1608.
10. Shanks K, Senthilarasu S, Mallick TK. High-concentration optics for photovoltaic applications. In: Pérez-Higueras P, Fernández E, editors. High Concentrator Photovoltaics: Fundamentals, Engineering and Power Plants. Cham, Switzerland: Springer; 2015; pp. 85–113.
11. Fernández-Reche J, Cañadas I, Sánchez M, Ballestrín J, Yebra L, Monterreal R, Rodríguez J, García G, Alonso M, Chenlo F. PSA solar furnace: a facility for testing PV cells under concentrated solar radiation. Solar Energy Mater Solar Cells. 2006; 90 (15): 2480–2488.
12. Pérez-Higueras P, Ferrer-Rodríguez JP, Almonacid F, Fernández EF. Efficiency and acceptance angle of high concentrator photovoltaic modules: current status and indoor measurements. Renew Sustain Energy Rev. 2018; 94: 143–153. doi: 10.1016/j.rser.2018.06.011.
13. Hadavinia H, Singh H. Modelling and experimental analysis of low concentrating solar panels for use in building integrated and applied photovoltaic (BIPV/BAPV) systems. Renew Energy. 2019; 139: 815–829.
14. Chemisana D. Building integrated concentrating photovoltaics: a review. Renew Sustain Energy Rev. 2011; 15 (1): 603–611.
15. Chemisana D, Ibáñez M, Barrau J. Comparison of Fresnel concentrators for building integrated photovoltaics. Energy Conversion Manage. 2009; 50 (4): 1079–1084.
16. Baig H, Heasman KC, Mallick TK. Non-uniform illumination in concentrating solar cells. Renew Sustain Energy Rev. 2012; 16 (8): 5890–5909.
17. Amanlou Y, Hashjin TT, Ghobadian B, Najafi G, Mamat R. A comprehensive review of uniform solar illumination at low concentration photovoltaic (LCPV) systems. Renew Sustain Energy Rev. 2016; 60: 1430–1441.
18. Jahanfar A, Drake J, Sleep B, Margolis L. Evaluating the shading effect of photovoltaic panels on green roof discharge reduction and plant growth. J Hydrol. 2019; 568: 919–928.
19. Bernadette D, Twizerimana M, Bakundukize A, Pierre BJ, Theoneste N. Analysis of shading effects in solar PV system. Int J Sustain Green Energy. 2021; 10 (2): 47–62.
20. Bayrak F, Ertürk G, Oztop HF. Effects of partial shading on energy and exergy efficiencies for photovoltaic panels. J Cleaner Prod. 2017; 164: 58–69.
21. Mandalaki M, Papantoniou S, Tsoutsos T. Assessment of energy production from photovoltaic modules integrated in typical shading devices. Sustain Cities Soc. 2014; 10: 222–231.
22. Xu S, Zhu Q, Hu Y, Zhang T. Design and performance research of a new non-tracking low concentrating with lens for photovoltaic systems. Renew Energy. 2022; 192: 174–187.
23. Mallick TK, Eames PC. Electrical performance evaluation of low-concentrating non-imaging photovoltaic concentrator. Prog Photovoltaics Res Appl. 2008; 16 (5): 389–398.
24. Chong KK, Siaw FL, Wong CW, Wong GS. Design and construction of non-imaging planar concentrator for concentrator photovoltaic system. Renew Energy. 2009; 34 (5): 1364–1370.
25. Andrews RW, Pollard A, Pearce JM. Photovoltaic system performance enhancement with non-tracking planar concentrators: experimental results and BDRF based modelling. In: 2013 IEEE 39th Photovoltaic Specialists Conference (PVSC), Tampa, FL, USA, June 16–21, 2013. pp. 0229–0234.
26. Buni MJ, Al-Walie AA, Al-Asadi KA. Effect of solar radiation on photovoltaic cell. Int Res J Adv Eng Sci. 2018; 3 (3): 47–51.
27. Amelia AR, Irwan YM, Leow WZ, Irwanto M, Safwati I, Zhafarina M. Investigation of the effect temperature on photovoltaic (PV) panel output performance. Int J Adv Sci Eng Inform Technol. 2016; 6 (5): 682–688.
28. Armenta-Déu C. Analysis of the performance of a PV-PCM system in variable solar radiation conditions. J Alternate Energy Sources Technol. 2021; 12 (1): 1–20. doi: 10.37591/joaest.v12i1.4423.

 

29. Duffie JA, Beckman WA. Solar Engineering of Thermal Processes. 3rd edition. New York, NY, USA: John Wiley & Sons; 2006.
30. Armenta-Déu C. Compact PV-PCM system with heat recovery unit for cogeneration system. J Alternate Energy Sources Technol. 2023; 14 (1): 13–24.

 